Agricultural and Forest Meteorology, 61 (1992) 129-149
Elsevier Science Publishers B.V., Amsterdam

Energy transfer over crop canopies: simulation and experimental verification

R.F. Grant[a] and D.D. Baldocchi[b]

[a]*Department of Soil Science, University of Alberta, Edmonton, Alta., T6G 2E3, Canada*
[b]*Atmospheric Turbulence and Diffusion Division, NOAA, P.O. Box 2456, Oak Ridge, TN 37831, USA*

(Received and accepted 6 November 1991)

ABSTRACT

Grant, R.F. and Baldocchi, D.D., 1992. Energy transfer over crop canopies: simulation and experimental verification. Agric. For. Meteorol., 61: 129-149.

The exchange of energy between the atmosphere and the surfaces of crops and soils stabilizes the thermal regimes at these surfaces, allowing sustained biological activity to occur. In this study, a simple Eulerian submodel of energy exchange was constructed from published algorithms in order to reproduce the dynamics of water and energy exchange between the soil–crop surface and the atmosphere as part of a larger agroecosystem model. Hourly output from the submodel was compared with data recorded over a soybean (*Glycine max*. L. Merr.) canopy at Mead, Nebraska on two dates during which soil water status differed. Recorded diurnal trends of leaf water potential and leaf stomatal resistance were reproduced in simulated diurnal trends of canopy water potential and canopy stomatal resistance on both dates. Under water stress, simulated canopy water potential was 0.1–0.2 MPa higher, and simulated canopy stomatal resistance approximately 25% lower, than recorded leaf values. Simulated fluxes of net radiative energy, and of latent, sensible, and soil heat were within 50 W m^{-2} of recorded values. Differences between simulated canopy and recorded air temperatures were consistent with those calculated at other sites under comparable atmospheric conditions. Inclusion of these algorithms in the agroecosystem model allowed a more comprehensive validation of the simulated transport of water and energy through the agroecosystem than would otherwise be possible.

INTRODUCTION

Radiative energy received from the sun and the atmosphere is exchanged for latent and sensible heat by crop and soil surfaces. The relative amounts of latent and sensible heat exchanged by these surfaces are understood to be mediated by resistance to water movement in aqueous and vapor phases between the crop or soil and the atmosphere. Through this exchange, the thermal and hydrologic regimes of the crop and soil are stabilized, allowing

---

Correspondence to: R.F. Grant, Department of Soil Science, University of Alberta, Edmonton, Alta., T6G 2E3, Canada.

biological activity to be sustained. If these regimes are to be reproduced mathematically in ecological simulation models, then the processes through which energy exchange occurs should be explicitly represented.

In more detailed models of energy exchange the crop canopy is resolved spatially into horizontal layers (e.g. Shawcroft et al., 1974), or biologically into sunlit and shaded leaf fractions (e.g. Norman, 1982) for each of which the transfer of short wave and thermal radiation, of latent and sensible heat, and of CO_2 is calculated. The transfer of radiation through the canopy is based upon the interception, reflection and transmission of direct and diffuse solar irradiance by leaf surfaces defined by height, azimuth and inclination within the canopy. The transfer of latent and sensible heat and of CO_2 through the canopy is based upon vertical gradients of humidity, temperature and CO_2 concentration, and upon eddy diffusion coefficients. Validation of model output with vertical profiles of net radiation, humidity, temperature, CO_2 and wind speed allows a rigorous test of fundamental hypotheses about energy transfer. However, such data are difficult and expensive to collect over the wide range of conditions necessary for such validation.

Considerable simplification of such models may be achieved by assuming that eddy diffusion within the canopy is high, so that vertical profiles of humidity, temperature, CO_2 and wind speed are relatively uniform. The validity of this assumption is supported by detailed Lagrangian random walk models (Baldocchi, 1990). In these simplified models, the canopy is treated as being within a single air layer for purposes of latent and sensible heat exchange. Output from single and multi-layered models have been observed to be within 10% for daily fluxes of transpiration (Sinclair et al., 1976) and within 2% for short-term fluxes of latent and sensible heat (De Wit, 1978). The use of a single air layer within the canopy has therefore been considered to be reasonable for closed canopies. For open canopies, an additional layer is required in the model for energy exchange between the soil surface and the crop–atmosphere.

An important application of the simulation of energy exchange is the estimation of canopy temperature and transpiration under changing soil and atmospheric conditions. In this application, the inter-relationship is simulated between atmospheric energy exchange and canopy water status, mediated by the effects of soil and canopy water status on resistance to the transport of water in liquid and vapor phases. The canopy water status in turn influences its rate of CO_2 assimilation, and consequently its growth, and is thus of considerable agronomic interest. However, in earlier attempts to simulate canopy water status (e.g. Zur and Jones, 1981; Hoogenboom et al., 1987; Grant, 1990a) the canopy energy exchange has not been explicitly represented. In order to represent the linkages between water movement and energy transfer within the soil–crop–atmosphere system, the simulation model of Grant (1990a) was extended to include a more comprehensive treatment of radiative energy and latent heat transfer through the atmosphere, canopy, and soil surface, as well as a treatment of sensible heat transfer and canopy temperature. This extension involved the integration into the model of several interrelated algorithms from the literature in which separate processes of water and energy transfer within the ecosystem are described. The objective of this study was to examine the behavior of a first order Eulerian submodel of water and energy exchange linked to a submodel of soil–crop hydrology. The extent to which the combined submodels could reproduce diurnal trends in atmospheric energy exchange and canopy water status was determined from data recorded over a soybean canopy at different levels of soil water deficit.

MATERIALS AND METHODS

Simulation Model

The exchange of energy between crop canopies and the atmosphere is simulated from hourly meterological data for solar irradiance, air temperature, humidity, wind speed and precipitation. In this simulation, the canopy is resolved into horizontal layers for irradiance interception, but is considered as a single layer for latent and sensible heat transfer. Calculation of exchange fluxes between the canopy leaf surfaces and the atmosphere is based upon the solution of the energy balance equation

$$R_{\mathrm{nc}} + LE_{\mathrm{c}} + CP_{\mathrm{c}} + LV_{\mathrm{c}} + H_{\mathrm{c}} + S_{\mathrm{c}} = 0 \tag{1}$$

where: R_{nc} is net irradiance retained by the canopy; LE_{c} is latent heat flux; CP_{c} is thermal energy of precipitation flux retained as free water on crop leaf surfaces; LV_{c} is latent heat of evaporation from free water on crop leaf surfaces; H_{c} is sensible heat flux; S_{c} is change in thermal energy stored in phytomass; all MJ m^{-2} ground area h^{-1}.

R_{nc} in eqn. (1) is calculated as

$$R_{\mathrm{nc}} = R_{\mathrm{c}} + F_{\mathrm{c}}R_{\mathrm{ly}} + F_{\mathrm{c}}R_{\mathrm{lg}} + R_{\mathrm{lc}} \tag{2}$$

where: R_{c} is shortwave irradiance absorbed by the canopy; R_{ly} is thermal emittance from the sky; R_{lg} is thermal emittance from the ground surface; R_{lc} is thermal emittance from the canopy; F_{c} is fraction of emitted energy intercepted by the canopy (m^2 canopy area m^{-2} ground area).

R_{c} in eqn. (2) is calculated as

$$R_{\mathrm{c}} = \sum_{k=1}^{K}\sum_{l=1}^{L}\sum_{m=1}^{M}\{(R_{\mathrm{bl}(k,l,m)} + R_{\mathrm{dl}(k,l,m)})A_{\mathrm{b}(k,l,m)} + R_{\mathrm{dl}(k,l,m)}(A_{(k,l,m)} - A_{\mathrm{b}(k,l,m)})\} \tag{3}$$

where: k is horizontal canopy layer number (1 is lowest; K is highest); l is leaf azimuth class number; m is leaf inclination class number; $R_{\mathrm{b1}(k,l,m)}$ is direct shortwave irradiance absorbed by leaf surface k,l,m;$R_{\mathrm{d1}(k,l,m)}$ is diffuse shortwave irradiance absorbed by leaf surface k, l, m; $A_{\mathrm{b}(k,l,m)}$ is area of leaf surface k, l, m exposed to $R_{\mathrm{b1}(k,l,m)}$ ($\mathrm{m^2\,m^{-2}}$); $A_{(k,l,m)}$ is total area of leaf surface k, l, m ($\mathrm{m^2\,m^{-2}}$).

$R_{\mathrm{b1}(k,l,m)}$ in eqn. (3) is calculated as

$$R_{\mathrm{b1}(k,l,m)} = (1-\alpha_{\mathrm{r}})(1-\tau_{\mathrm{r}})R_{\mathrm{b}}|\cos\theta_{(k,l,m)}| \tag{4}$$

where: α_{r} is shortwave albedo; τ_{r} is shortwave transmission coefficient; R_{b} is shortwave irradiance in the direction of the solar beam; $\theta_{(k,l,m)}$ is incident angle of R_{b} on $A_{\mathrm{b}(k,l,m)}$ (rad) (Grant et al., 1989a).

$R_{\mathrm{d1}(k,l,m)}$ in eqn. (3) is calculated as

$$R_{\mathrm{d1}(k,l,m)} = \sum_{n=1}^{N} R_{\mathrm{d1}(k,l,m,n)} \tag{5}$$

where: n is sky zone number and

$$R_{\mathrm{d1}(k,l,m,n)} = (1-\alpha_{\mathrm{r}})(1-\tau_{\mathrm{r}})R_{\mathrm{d}(n)}|\cos\lambda_{(l,m,n)}|\left\{1-\sum_{j=k+1}^{K} F_{\mathrm{d}(j)}\right\} \tag{6}$$

where: $R_{\mathrm{d}(n)}$ is shortwave irradiance in the direction of sky zone n; $\lambda_{(l,m,n)}$ is incident angle of $R_{\mathrm{d}(n)}$ on $A_{(k,l,m)}$ (rad) (Grant et al., 1989a); $\Sigma_{j=k+1}^{K} F_{\mathrm{d}(j)}$ is fraction of R_{d} absorbed by all layers $j > k$.

R_{b} in eqn. (4) and $R_{\mathrm{d}(n)}$ in eqn. (6) are calculated from total shortwave irradiance recorded on a horizontal surface (R_{r}) (Grant et al., 1989a).

$A_{\mathrm{b}(k,l,m)}$ in eqn. (3) is calculated as

$$A_{\mathrm{b}(k,l,m)} = A_{(k,l,m)}\left\{1-\sum_{j=k+1}^{K} F_{\mathrm{b}(j)}\right\} \tag{7}$$

where: $\Sigma_{j=k+l}^{K} F_{\mathrm{b}(j)}$ = fraction of R_{b} absorbed by all layers $j > k$.

Each F_{b} in eqn. (7) is calculated as

$$F_{\mathrm{b}(k)} = \sum_{l=1}^{L}\sum_{m=1}^{M}(1-\alpha_{\mathrm{r}})(1-\tau_{\mathrm{r}})\{A_{(k,l,m)}[1-(1-|\cos\theta_{(l,m,n)}|^{(1/\sin\beta_{\mathrm{b}})})]\} \times\left\{1-\sum_{j=k+1}^{K} F_{\mathrm{b}(j)}\right\} \tag{8}$$

where: β_{b} is inclination of sun (rad).

Each $F_{\mathrm{d}(k)}$ in eqn. (6) is calculated as

$$F_{\mathrm{d}(k)} = \sum_{l=1}^{L}\sum_{m=1}^{M}\sum_{n=1}^{N}(1-\alpha_{\mathrm{r}})(1-\tau_{\mathrm{r}})/N\{A_{(k,l,m)}[1-(1-|\cos\sigma_{(l,m,n)}|^{(1/\sin\beta_{\mathrm{d}(n)})})]\} \times\left\{1-\sum_{j=k+1}^{K} F_{\mathrm{d}(j)}\right\} \tag{9}$$

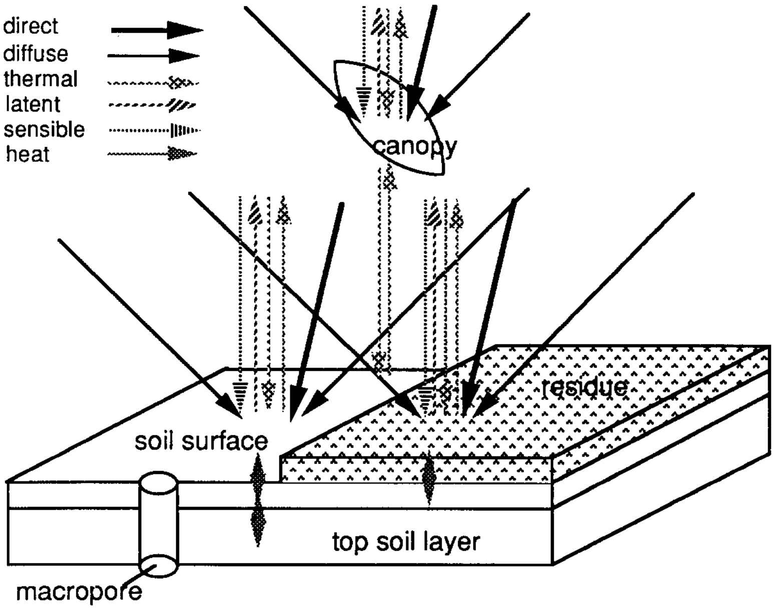

Fig. 1. Energy transfer processes through the soil–crop–atmosphere system represented in the simulation model. Abbreviations as in text.

where: $\beta_{\mathrm{d}(n)}$ is inclination of sky zone n (rad).

F_c in eqn. (2) is approximated as

$$F_c \approx \sum_{k=1}^{K} F_{\mathrm{d}(k)} \tag{10}$$

on the assumption that the absorption of emitted thermal energy is similar to that of shortwave irradiance.

R_{ly} in eqn. (2) is calculated from sky emissivity (Sellers, 1965), air temperature and vapor content, R_{lg} is calculated from the emissivities, temperatures (Van Bavel and Hillel, 1976) and fractional exposures (Grant et al., 1990) of soil and residue surfaces, and R_{lc} is calculated from the canopy emissivity and temperature

$$R_{\mathrm{lc}} = F_c \varepsilon_c \sigma T_c^4 \tag{11}$$

where: ε_c is canopy emissivity; σ is Stefan–Boltzmann constant (MJ $\mathrm{m^{-2} h^{-1} K^{-4}}$); T_c is canopy temperature (K) on the assumption that the fractional emittance of thermal energy per unit ground area by the canopy may be approximated as the fractional interception of diffuse irradiance. Energy fluxes among the atmosphere, canopy and soil surface are represented diagrammatically in Fig. 1.

LE_c in eqn. (1) is calculated as

$$LE_c = F_c L v (q_a - q_c)/(r_a + r_c) \tag{12}$$

where: L is latent heat of water evaporation (MJ m^{-3}); υ is specific volume of water (m^3 Mg^{-1}); q_a is vapor density (Mg m^{-3}) at T_a (air temperature in K); q_c is vapor density (Mg m^{-3}) at T_c; r_a is canopy boundary layer resistance to vapor transport (h m^{-1}); r_c is canopy stomatal resistance to vapor transport (h m^{-1}) on the assumption that the fractional emission of latent energy per unit ground area by the canopy may be approximated as the fractional interception of diffuse irradiance. The value of q_a is calculated from recorded T_a and vapor pressure (e_a in kPa) or relative humidity (RH). Canopy vapor flux (E_c in m^3 m^{-2} h^{-1}) is calculated as LE_c/L.

The term r_a in eqn. (12) represents the sum of the resistance to momentum transfer and the resistance of the quasi-laminar boundary layer, calculated as

$$r_a = \{(\ln((z_a + z_c)/z_c)\ln((z_a + z_v)/z_v)/(K^2 U_a)\}/(1.0\text{–}10.0\ Ri) \quad (13)$$

where: z_a is height above the zero plane displacement height at which wind speed is recorded (m); z_c is momentum roughness parameter (m) equal to 0.125 of the canopy height, calculated in the model from the simulated lengths of individual leaves, petioles and internodes; z_v is vapor roughness parameter (m) equal to 0.2 of z_c (Campbell, 1977); K is Von Karman constant; U_a is wind speed recorded at z_a(m h^{-1}); Ri is the Richardson number calculated from $T_c - T_a$ and U_a according to Van Bavel and Hillel (1976).

The term r_c in eqn. (12) is calculated as an empirical function of the canopy turgor Ψ_t (MPa)

$$r_c = r_c(\mathrm{mn}) + (r_c(\mathrm{mx}) - r_c(\mathrm{mn}))\, e^{(-13.7\Psi_t)} \quad (14)$$

(Zur and Jones, 1981) where $r_{c(mn)}$ is r_c when Ψ_c (canopy water potential in MPa) $= 0$; $r_{c(mx)}$ is r_c when $\Psi_t = 0$.

The value of $r_{c(mx)}$ is set to represent cuticular resistance to water vapor transfer when stomata are closed. The term Ψ_t in eqn. (14) is a function of Ψ_c

$$\Psi_t = \Psi_{t(mx)} + \omega\Psi_c \quad (15)$$

where: $\Psi_{t(mx)}$ is Ψ_t when $\Psi_c = 0$ (1.2 MPa); ω is the osmotic adjustment coefficient (0.6 MPa MPa^{-1}) (Grant and Lea, 1981), such that canopy osmotic potential (Ψ_π) in MPa) $= \Psi_c - \Psi_t$.

The value of $r_{c(mn)}$ in eqn. (14) is calculated from the simulated rate of canopy CO_2 assimilation under ambient irradiance, temperature, CO_2 and non-limiting water. First, the total canopy resistance to gaseous diffusion of CO_2($r_c CO_{2(mn)}$ in h m^{-1} ground area) is calculated

$$r_c CO_{2(mn)} = (C_o - C_i)/(Q_c/F_c) \quad (16)$$

where: C_o is ambient CO_2 concentration (μmol m^{-3}); C_i is intercellular CO_2 concentration (μmol m^{-3}); Q_c is rate of canopy CO_2 assimilation (μmol m^{-2} ground area h^{-1}) at current CO_2, irradiance and temperature on the assumption that the fractional uptake of CO_2 per unit ground area by the canopy may be approximated as the fractional interception of diffuse irradiance. The value of Q_c in eqn. (16) is calculated as the sum of those for its leaf surfaces (Grant, 1989a; Grant et al., 1989a). Algorithms for the interception of photosynthetic irradiance are the same as those for total shortwave irradiance (eqns. (3)–(9)), but use α_p and τ_p (albedo and transmission coefficients for photosynthetic irradiance) in place of α_r and τ_r (Eqns. (4) and (6)).

The value of $r_c CO_{2(mn)}$ in eqn. (16) is then used to calculate $r_{c(mn)}$ in eqn. (14)

$$r_{c(mn)} = (r_c CO_{2(mn)} - 1.4\, r_a)/1.6 \tag{17}$$

where 1.4 and 1.6 are the ratios for boundary layer and stomatal resistances to the diffusive transfer of CO_2 and water. The value of r_c in eqn. (14) thus reflects both the photosynthetic and the water status of the canopy.

CP_c in eqn. (1) is calculated as

$$CP_c = C_w T_a P_c \tag{18}$$

where: C_w is volumetric heat capacity of water (MJ m^{-3} °C^{-1}); P_c is precipitation flux retained in a free water pool on canopy leaf surfaces (m^3 m^{-2} h^{-1}); P_c is calculated from P, the precipitation flux, and from canopy LAI according to Shaffer and Larson (1987).

LV_c in eqn. (1) is calculated as is LE_c in eqn. (12), but without r_c

$$LV_c = F_c L\upsilon(q_a - q_c)/r_a \tag{19}$$

Vapor flux from the free water pool (V_c in m^3 m^{-2} h^{-1}) is calculated from LV$_c$ as is E_c from LE_c. The latent flux in eqn. (1) occurs as LV_c ($LE_c = 0$) if free water is present, and as LE_c ($LV_c = 0$) if absent. If $LE_c > 0$ (condensation) E_c occurs as V_c.

H_c in eqn. (1) is calculated as

$$H_c = F_c C_a (T_a - T_c)/r_a \tag{20}$$

where: C_a is volumetric heat capacity of air (MJ m^{-3} °C^{-1}) on the assumption that the fractional emission of sensible heat per unit ground area by the canopy may be approximated as the fractional interception of diffuse irradiance.

S_c in eqn. (1) is calculated as

$$S_c = C_c (T_{c(j-1)} - T_{c(j)}) \tag{21}$$

where: C_c is areal heat capacity of the canopy (MJ m^{-2} K^{-1}); j is current time step (h); $j - 1$ is previous time step (h); C_c is estimated from υ, C_w and from canopy phytomass and water content (Mg m^{-2}). The value of $T_{c(j)}$ is still unknown. If from eqn. (1)

$$H_c + S_c = -(R_{nc} + LE_c + CP_c + LV_c) \tag{22}$$

and if from eqns. (20) and (21)

$$H_c + S_c = F_c C_a (T_{a(j)} - T_{c(j)})/r_a + C_c (T_{c(j-1)} - T_{c(j)}) \tag{23}$$

then

$$T_{c(j)} = (F_c C_a T_{a(j)}/r_a + C_c T_{c(j-1)} + R_{nc} + LE_c + CP_c + LV_c)/(C_c + F_c C_a/r_a) \tag{24}$$

H_c is then solved from $T_{c(j)}$ (eqn. (20)), allowing S_c to be calculated from eqn. (21). T_c (eqn. (24) is used to calculate R_{1c} and hence R_{nc} (eqn. (2)), as well as q_s and hence LE_c (eqn. (12)) and LV_c (eqn. (19)).

Water uptake by the crop root system (U_c in $m^3 m^{-2} h^{-1}$) is calculated as the sum of that from each horizontal soil layer k within which roots have grown ($U_{c(k)}$ in $m^3 m^{-2} h^{-1}$). Assuming negligible capacitance in the root system $U_c(k)$ is equal both to the radial water flux from the soil to the root surface ($U_{s(k)}$) and to the axial water flux from the root surface to the canopy ($U_{r(k)}$), where

$$U_{s(k)} = (\Psi_{r(k)} - \Psi_{s(k)})/r_{g(k)} \tag{25}$$

and

$$U_{r(k)} = (\Psi_c - \Psi_{r(k)})/\mathrm{r}_{r(k)} \tag{26}$$

in which: $\Psi_{r(k)}$ is the water potential of the roots in layer k (MPa); $\Psi_{s(k)}$ is that of the soil in layer k (MPa) (Grant, 1990a); $\mathrm{r}_{g(k)}$ is the soil hydraulic resistance to radial flow in layer k (MPa h m^{-1}); $r_{r(k)}$ is the root hydraulic resistance to axial flow in layer k (MPa h m^{-1}).

The term $r_{g(k)}$ in eqn. (25) is calculated as

$$r_{g(k)} = \{\ln(\mathrm{d}_{2(k)}/\mathrm{d}_{1(k)})/2\pi K_{s(k)} L_{r(k)})\}\theta_{p(k)}/\theta_{w(k)} \tag{27}$$

where: $d_{2(k)}$ is mean distance between adjacent roots (m); $d_{1(k)}$ is root radius (m); $K_{s(k)}$ is mean hydraulic conductivity along radial flow path ($m^2 h^{-1} MPa^{-1}$); $L_{r(k)}$ is root length per unit ground area in layer k ($m\,m^{-2}$); $\theta_{p(k)}$ is soil porosity ($m^3 m^{-3}$); $\theta_{w(k)}$ is soil water content ($m^3 m^{-3}$).

The value of $d_{2(k)}$ is calculated from root length density ($L_{d(k)}$ in $m\,m^{-3}$) according to Gardner (1960). $L_{d(k)}$ arises from the crop growth submodel (Grant, 1989b, 1990a,b). $K_{s(k)}$ is calculated as the inverse of the average hydraulic resistivity at $\Psi_{r(k)}$ and $\Psi_{s(k)}$, calculated according to Green and Corey (1971). Use of the term $\theta_{p(k)}/\theta_{w(k)}$ was suggested by Herkelrath et al. (1977) to account for the root surface not in contact with water-filled soil pores.

The term $r_{r(k)}$ in eqn. (26) is calculated as

$$r_{r(k)} = 1.0/(K_r L_{r(k)}) \tag{28}$$

where: K_r is specific root conductivity ($1.8 \times 10^{-8} m^3 h^{-1} MPa^{-1}$ m per root) estimated from data presented by De Willigen and van Noordewijk (1987). If $U_{s(k)} = U_{r(k)}$, then $\Psi_{r(k)}$ may be calculated as

$$\Psi_{r(k)} = (\Psi_{s(k)} r_{r(k)} + \Psi_c \mathrm{r}_{g(k)})/(r_r(k) + r_{g(k)}) \tag{29}$$

from which eqns. (25) and (26) are solved.

Hourly values of E_c from eqn. (12) and U_c from eqns. (25) and (26) are equilibrated by converging upon a value of Ψ_c with an acceptance criterion of 0.001. Equations (1)–(2) and (11)–(29) are solved within each convergence cycle to arrive at a solution in which all components of the canopy–atmosphere energy balance and the soil–canopy water potential gradient are consistent.

The simulation of energy exchange over the soil and residue surfaces (Fig. 1) is based on the conservation of energy over each surface. Thus over soil

$$R_{ns} + LE_s + CP_s + LV_s + H_s + S_s = 0 \qquad (30)$$

where each term corresponds to one over the canopy, and the subscript s refers to the soil surface. The calculation of each flux in eqn. (30) is analogous to that in eqn. (1), and is described in detail elsewhere (Grant et al., 1990). In the agroecosystem model, the soil surface is represented as a surface layer of 0.01 m depth overlying a multilayered soil profile through which heat and water are transported vertically. The calculation of the surface temperature used in the calculation of these fluxes thus arises from net heat exchange between the atmosphere, the soil surface, and the soil layer below.

These algorithms function within an agroecosystem simulation model where they provide hourly estimates of energy exchange and consequent movement of water and heat through the canopy and soil profile. Water and heat status arising from these estimates are used elsewhere in the model as inputs to biological algorithms describing microbial, root and shoot behavior. The agroecosystem model is constructed such that a crop may or may not be present during model execution. If a crop species is specified, values for species-specific characteristics taken from the scientific literature are read by the model from an external file, causing the model to reproduce the development and growth patterns of the indicated crop species. The development and growth of soybeans is based on the phenology subroutine of Acock et al. (1985) linked to the photosynthesis submodel of Grant (1989a) and Grant et al. (1989a) and to an adaptation of the partitioning submodel of Grant (1989b) and Grant et al. (1989b).

Field Experiment

Normal (HD) and pubescent (HPD) isolines of soybeans (*Glycine max.* L. Merr. cv. 'Harosoy') were planted in an unirrigated 150 × 210 m field on a Sharpsburg silty clay loam (Typic Argiudoll — Table 1) at Mead, NE (41°N) during mid-May, 1980. On selected days during the growing season, vertical profiles were recorded hourly over the crop canopy of air temperature and vapor pressure (aspirated psychrometer; Rosenberg and Brown, 1974), wind speed (Cayuga, Ithaca, NY three-cup anemometers model WP-1)[1], and CO_2

---

[1] Commercial products mentioned by name do not imply endorsement by the University of Alberta or the NOAA to the exclusion of other suitable products.

TABLE 1

Physical characteristics of the Sharpsburg silty clay loam at Mead, NE. Data from Garay (1981)

Layer	1	2	3	4	5	6
Depth	0.15	0.30	0.60	0.90	1.20	1.50
BD ($\mathrm{Mg\,m^{-3}}$)	1.31	1.37	1.42	1.41	1.33	1.28
FC ($\mathrm{m^3\,m^{-3}}$)	0.41	0.43	0.42	0.40	0·39	0.37
WP ($\mathrm{m^3\,m^{-3}}$)	0.22	0.26	0.24	0.21	0.20	0.19
K_{sat} ($\mathrm{mm\,h^{-1}}$)	5.0	5.0	5.0	5.0	7.5	10.0
Sand (%)	6.0	4.4	7.0	4.9	3.0	5.8
Silt (%)	56.4	53.1	54.2	61.3	64.2	67.1
Clay (%)	33.9	38.5	36.7	33.4	31.5	26.4

concentration (Beckman infrared gas analyzer model 315A and 315B). Also recorded hourly were global radiation (Eppley, Newport, RI pyranometer model 8-48a), and net radiation (Swissteco, Melbourne, Vic. net radiometer type S-1) over the canopy, leaf water potential Ψ_l (Soil Moisture Equipment Corp., Santa Barbara, CA pressure chamber model 3005) and leaf stomatal resistance r_l (Lambda, Lincoln, NE Instruments steady-state porometer model LI-1600, of exposed leaves near the top of the canopy, and soil surface heat flux (Concept Engineering Old Saybrook, CT) heat flux plate model F-080-4) below the canopy. Crop height and LAI (Hayashi-Denco, Japan automatic area meter type AAM-5), and soil moisture content (Campbell Scientific, Logan, UT hydroprobe 503) were recorded weekly. Flux-gradient theory was used to calculate flux densities of latent and sensible heat from vertical gradient measurements. The Bowen energy balance method was used to calculate eddy exchange coefficients. Further information about instrument calibration, measurement techniques and energy flux calculations are given by Baldocchi (1982) and Baldocchi et al. (1983).

Model Validation

The agroecosystem model was run from 8 May to 19 August 1980, and simulated values for hourly energy fluxes among the soil surface, crop canopy and the atmosphere were compared with those recorded by Baldocchi (1982) on 24 July and 19 August 1980. Data for the physical characteristics of the soil used by the model were those recorded from the experimental site at Mead, NE (Table 1). Values of θ_w were initialized in the model at those of field capacity on 8 May. Data for R_r, T_a, U_a, and e_a recorded at the experimental site were used by the model for the two dates on which comparisons with recorded data were made. Because continuous meterological data were not available for the experimental site during 1980, hourly values for R_r T_a, U_a and e_a recorded during 1988 at Urbana, IL (Grant, 1989c) were used by the model for those dates on which comparisons with recorded data were not made.

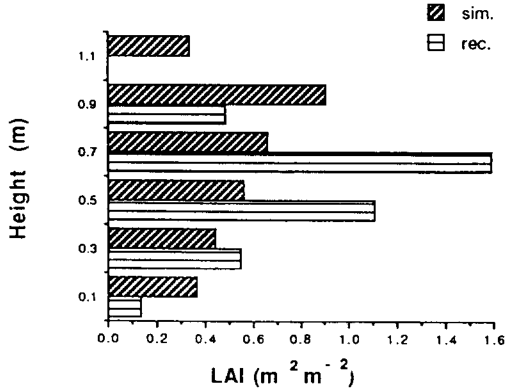

Fig. 2. Vertical distribution of soybean leaf area index (LAI) recorded and simulated at Mead, NE on 25 July 1980.

Simulated precipitation events during the growing season were used by the model to generate vertical profiles of θ_w close to those recorded prior to each of the two dates. Use of these data allowed the model to reproduce antecedent conditions of canopy stature and soil water content recorded at the experimental site on 24 July and 19 August, so that detailed comparisons with recorded energy fluxes could be made on these dates using site weather data.

For comparison with net radiation recorded over the soil–canopy surface, net radiation simulated on a horizontal plane (R_{nt} in $\mathrm{MJ\,m^{-2}h^{-1}}$) was calculated as

$$R_{nt} = F_{cbd}R_r + (1 - F_{cbd})(1 - \alpha_s)R_r + R_{ly} + F_cR_{lc} + (1 - F_c)R_{lg} \quad (31)$$

where: α_s is soil albedo; F_{cbd} is fractional interception of R_b and R_d, calculated as

$$F_{cbd} = R_c\Big/\left(R_b + \sum_{n=1}^{N} R_{d(n)}\right) \quad (32)$$

For comparison with latent and sensible fluxes recorded over the soil–canopy surface, total simulated latent (LE_t) and sensible (H_t) fluxes were calculated as

$$LE_t = LE_s + LE_c \quad (33)$$

and

$$H_t = H_s + H_c \quad (34)$$

RESULTS

Canopy height and LAI recorded on 24 July were 1.0 m and $3.85\,\mathrm{m^2\,m^{-2}}$ while those simulated were 1.1 and 3.28 (Fig. 2). Average canopy LAI

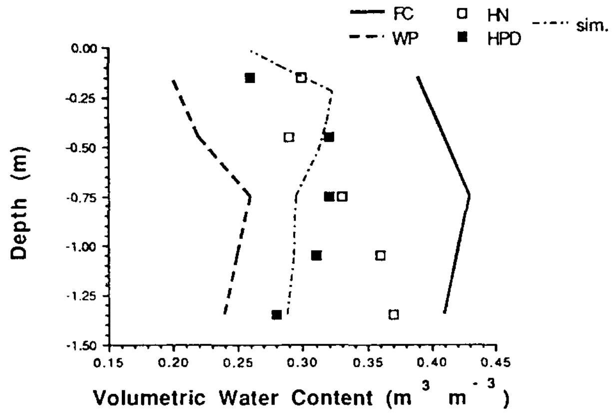

Fig. 3. Vertical distributions of volumetric water content through the soil profile recorded (symbols) under 'Harosoy' (HD) and 'Harosoy' pubescent (HPD) isolines and simulated (line) at Mead, NE on 25 July 1980. Also shown are vertical distributions of volumetric water content recorded through the soil profile at -0.03 MPa (FC) and -1.5 MPa (WP).

recorded on three dates during the week of 24 July was 3.52 $\mathrm{m}^2\,\mathrm{m}^{-2}$, indicating some variability in measurement. Simulated precipitation events allowed the model to reproduce the vertical profile of θ_w recorded under HPD on this date, but not he higher θ_w recorded below 0.90 m under HD (Fig. 3) in the same field. Under the meterological conditions recorded on 24 July (Figs. 4(a) and (b)), simulated Ψ_c declined from pre-dawn values of approximately -0.3 MPa to midafternoon values of approximately -1.4 MPa, and then recovered to post-sunset values of -0.3 MPa (Fig. 4(c)). Simulated Ψ_π declined from approximately -1.2 to -1.6 MPa during the day, and recovered to approximately -1.2 MPa the following night, as recorded experimentally on field grown soybeans by Reicocky et al. (1982). Simulated $\Psi_{\mathrm{r}(k)}$ in the upper four soil layers followed diurnal trends that integrated the effects of simulated Ψ_c and $\Psi_{\mathrm{s}(k)}$ (eqn. (29)). Simulated $\Psi_{\mathrm{r}(k)}$ in the top soil layer remained below Ψ_c after sunset. Under these conditions, $U_{\mathrm{s}(k)}$ (eqn. (25)) and $U_{\mathrm{r}(k)}$ (eqn. (26)) become positive, such that some redistribution of soil water occurs from soil layers with higher $\Psi_{\mathrm{s}(k)}$ to those with lower (Grant, 1990b). This phenomenon has been demonstrated experimentally by Baker and Van Bavel (1988). Values of Ψ_c simulated before sunrise reflected those of $\Psi_{\mathrm{r}(k)}$ and $\Psi_{\mathrm{s}(k)}$ simulated through the rooting zone when $r_{\mathrm{c(mn)}}$ is high (eqn. (17)) and $U_{\mathrm{r}(k)}$ and $U_{\mathrm{s}(k)}$ are low. Simulated Ψ_c and recorded Ψ_l were in close agreement before dawn, indicating that the vertical profile of $\Psi_{\mathrm{s}(k)}$ was reproduced with reasonable accuracy on this date. Daytime Ψ_l declined to lower values than did Ψ_c, but followed a similar diurnal trend.

The high LAI simulated on 24 July caused energy fluxes simulated at the soil surface to remain low (Fig. 4(d)), with R_ns rising from slightly negative

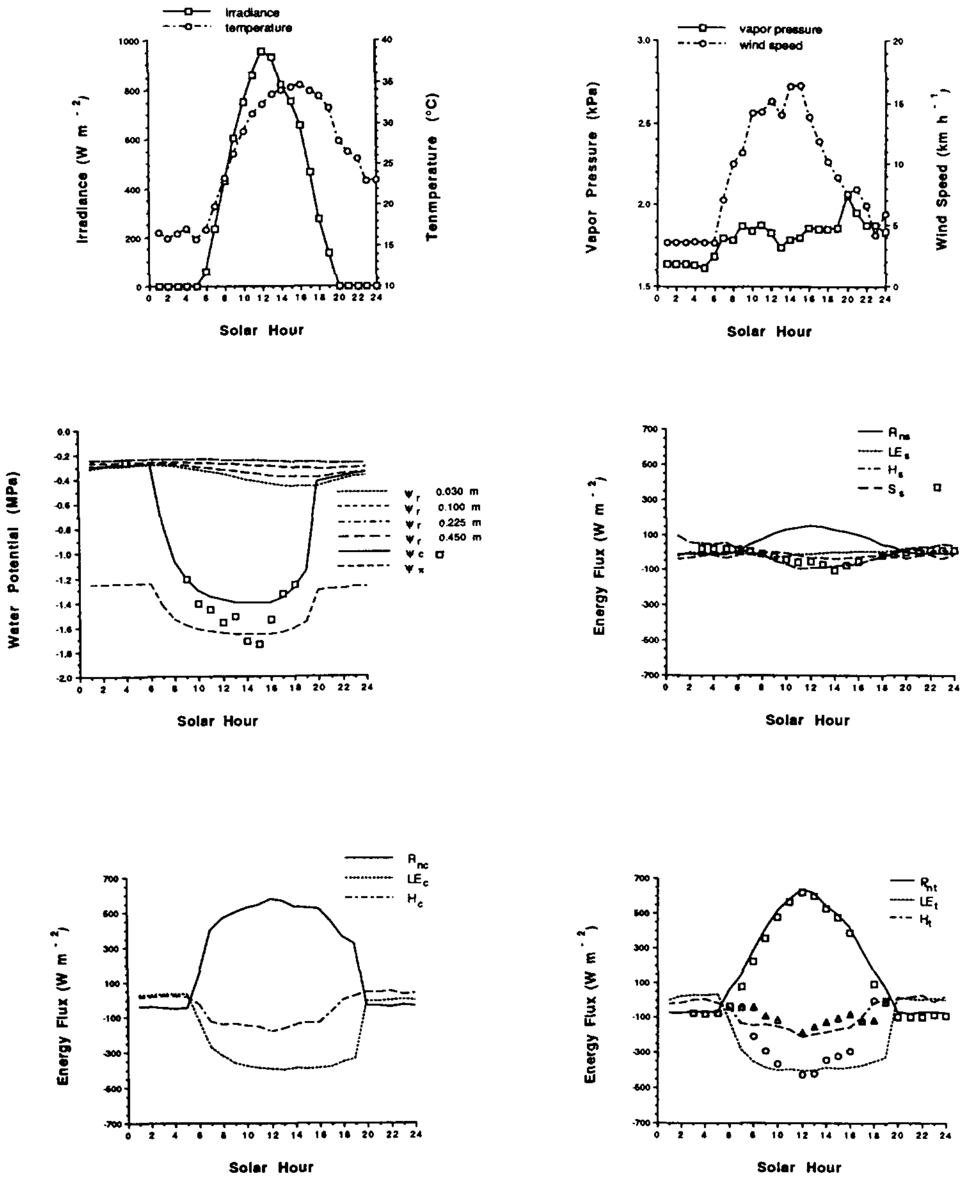

Fig. 4. (a) Irradiance and air temperature, (b) vapor pressure and wind speed recorded over the soybean canopy at Mead, NE on 24 July 1980. (c) Root (Ψ_r) and canopy (Ψ_c) water potentials simulated (lines) and leaf water potentials recorded (symbols) on the same date. (d) Net radiation (R_{ns}), and latent (LE_s), sensible (H_s) and heat (S_s) fluxes simulated (lines) and heat flux recorded (symbols) over the soil surface on the same date. (e) Net radiation (R_{nc}), and latent (LE_c) and sensible (H_c) heat fluxes simulated (lines) over the soybean canopy on the same date. (f) Total net radiation (R_{nt}), and latent (LE_t) and sensible (H_t) heat fluxes recorded (symbols) and simulated (lines) over the combined soil surface and soybean canopy on the same date. Standard differences between recorded and simulated data (MPa or $\mathrm{W\,m^{-2}}$): Ψ_c 0.17, S_s 23, R_{nt} 42, LE_t 163, H_t 69.

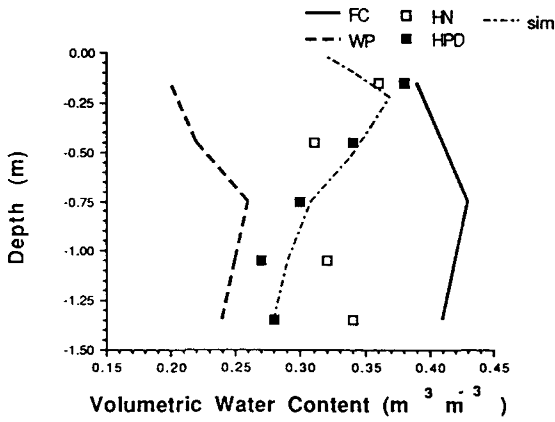

Fig. 5. Vertical distributions of volumetric water content through the soil profile recorded (symbols) under 'Harosoy' (HD) and 'Harosoy' pubescent (HPD) isolines and simulated (line) at Mead, NE on 19 August 1980. Also shown are vertical distributions of volumetric water content recorded through the soil profile at -0.03 MPa (FC) and -1.5 MPa (WP).

values during the night to approximately $100\,W\,m^{-2}$ during the day, while both LE_s and H_s remained low. S_s declined from approximately $50\,W\,m^{-2}$ during the night to approximately $-75\,W\,m^{-2}$ during the day, following recorded values. R_{nc} rose from $-75\,W\,m^{-2}$ before dawn to above $550\,W\,m^{-2}$ during mid-day (Fig. 4(e)), causing simulated LE_c and H_c to decline from approximately $25\,W\,m^{-2}$ before dawn to approximately $-400\,W\,m^{-2}$ and $-150\,W\,m^{-2}$ respectively during the day. R_{nt}, LE_t and H_t over both soil and crop surfaces were consistent with those recorded over the soybean canopy (Fig. 4(f)), except between 700 and 900 h and between 17:00 and 19:00 h when lower LE_t was simulated than was recorded. Simulated LE_t and H_t remained stable during the day, reflecting limitations to E_s and E_c imposed by higher crop and soil resistance (r_c in eqn. (12), r_g in eqn. (25) and r_r in eqn. (26)) to water movement.

Canopy height and LAI recorded on 19 August were 0.8 m (owing to lodging) and $3.42\,m^2\,m^{-2}$ while those simulated were 1.1 and 3.42. Average canopy LAI recorded on three dates during the week of 19 August was $3.15\,m^2\,m^{-2}$. The water content of the soil profile above 0.75 m was recharged between 24 July and 19 August (Fig. 5), while that below 0.9 m was slightly depleted. Simulated precipitation events allowed the model to reproduce the vertical profile of θ_w under *HPD* (Fig. 5) but not the higher θ_w recorded below 0.90 m under *HD* in the same field. Diurnal changes in R_t and T_a (Fig. 6(a)) recorded during 19 August were less than those recorded during 24 July (Fig. 4(a)) while e_a was higher (Fig. 6(b) vs Fig. 4(b)). As a consequence of higher θ_w and e_a recorded Ψ_l declined to approximately -1.0 MPa (Fig. 6(c)) vs. -1.7 MPa (Fig. 4(c)) on the earlier date. Simulated Ψ_c remained close to

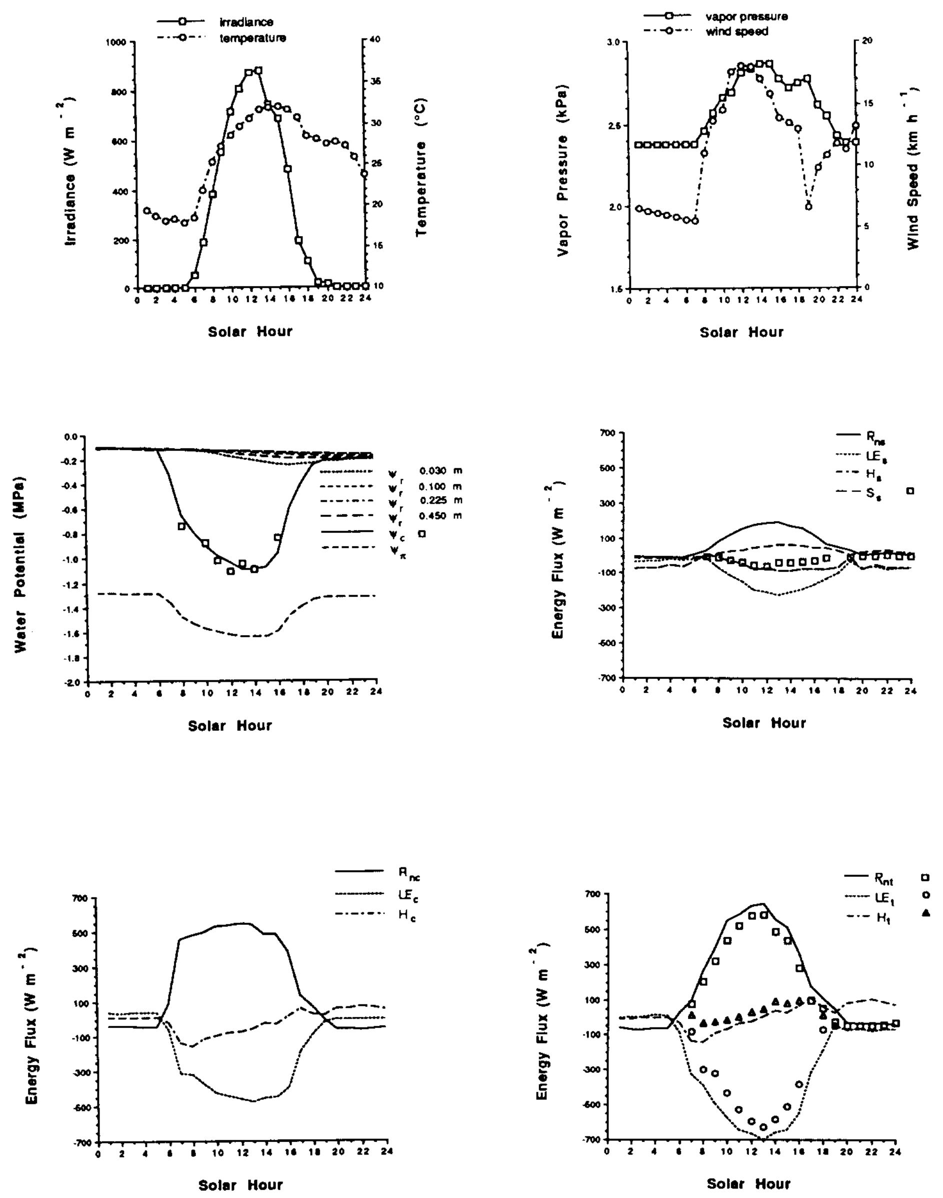

Fig. 6. (a) Irradiance and air temperature, (b) vapor pressure and wind speed recorded over the soybean canopy at Mead, NE on 19 August 1980. (c) Root (Ψ_r) and canopy (Ψ_c) water potentials simulated on the same date. (d) Net radiation (R_{ns}), and latent (LE_s), sensible (H_s) and heat (S_s) fluxes recorded (symbols; S_s only) and simulated (lines) over the soil surface on the same date. (e) Net radiation (R_{nc}), and latent (LE_c) and sensible (H_c) heat fluxes simulated (lines) over the soybean canopy on the same date. (f) Total net radiation (R_{nt}), and latent (LE_t) and sensible (H_t) heat fluxes recorded (symbols) and simulated (lines) over the combined soil surface and soybean canopy on the same date. Standard differences between recorded and simulated data (MPa or W m^{-2}): Ψ_c 0.13, S_s 47, R_{nt} 59, LE_t 132, H_t 73.

-0.1 MPa before dawn, in equilibrium with $\Psi_{r(n)}$ and $\Psi_{r(n)}$, and followed Ψ_l during the day.

Higher θ_w near the soil surface caused simulated LE_s to decline below $-150\,\mathrm{W\,m^{-2}}$ during mid-day, while simulated H_s rose above $50\,\mathrm{W\,m^{-2}}$, indicating transfer of heat to the soil surface (Fig. 6(d)). Simulated S_s declined to $-50\,\mathrm{W\,m^{-2}}$ during the day, as did recorded S_s. Simulated LE_c was lower and H_c higher on 19 August than on 24 July (Fig. 6(e)). The rise in H_c during the day was caused by the increase (in a negative sense) in LE_c relative to R_{nc} as T_a increased. The model reproduced the lower LE_t and higher H_t recorded on this date (Fig. 6(f)), as compared with those recorded earlier (Fig. 4f). LE_t followed a more sinusoidal trend than did that on 24 July, caused in the model by reduced constraints imposed by crop and soil resistances on E_s and E_c. R_{nc} was overestimated, and LE_t underestimated, during the day by approximately $50\,\mathrm{W\,m^{-2}}$.

Simulated r_c (eqn. (14)) during 24 July rose from early morning values of $80\,\mathrm{s\,m^{-1}}$ to mid-afternoon values of approximately $180\,\mathrm{s\,m^{-1}}$ before declining to approximately $100\,\mathrm{s\,m^{-1}}$ during early evening (Fig. 7(a)). Daytime values were lower than those of recorded r_l, as was found by Ben-Asher et al. (1989). Differences between r_c and r_l integrated over the canopy have also been observed by Baldocchi et al. (1987). Simulated r_a (eqn. (13)) declined from about $130\,\mathrm{s\,m^{-1}}$ to about $15\,\mathrm{s\,m^{-1}}$ as the simulated temperature profile over the canopy became lapse during the early morning, and increased to about $100\,\mathrm{s\,m^{-1}}$ as the profile became inverted during the night (Fig. 7(b)). Simulated r_c during 19 August remained close to $r_{c(mn)}$ (eqns. (16) and (17)), declining from about $200\,\mathrm{s\,m^{-1}}$ at dawn to about $55\,\mathrm{s\,m^{-1}}$ as Q_c increased during the day, and rising above $200\,\mathrm{s\,m^{-1}}$ as Q_c declined during the evening (Fig. 7(a)). Daytime values corresponded closely to recorded r_l. Simulated r_a remained low during the entire day, and was less influenced by simulated canopy–atmosphere temperature gradients (Fig. 7(b)) as gradients were lower and wind speeds higher (Fig. 6(b)) than those on 24 July.

DISCUSSION

Apart from the use of simulated precipitation data, no site adjustment of the model was undertaken in order to induce agreement between simulated and recorded data. However, uncertainty remains in the estimation of both radiative and turbulent components of the energy balance, requiring the use of some assumptions. The calculation of R_{nc} (eqn. (2)) is based on the interception of non-vertical irradiance by non-horizontal leaves, while that of R_{nt} (eqn. (31)) is based on interception by a horizontal surface. Consequently, simulated diurnal profiles of R_{nc}, and hence of LE_c, will be less sinusoidal than those of R_{nt} (e.g. Figs. 4(e) and (f)), and will be influenced by assumptions about the vertical and axial distributions of canopy leaf surfaces. Therefore

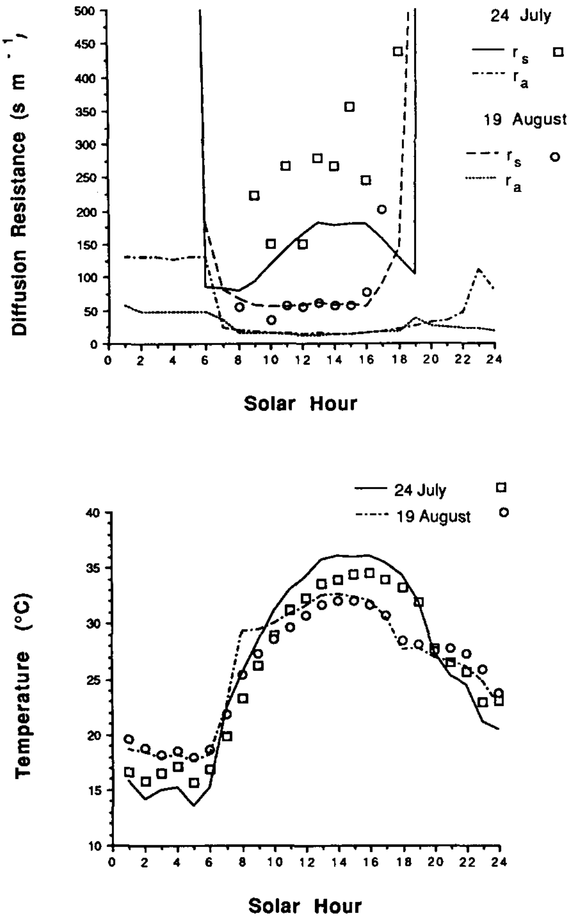

Fig. 7. (a) Canopy stomatal (r_c) and boundary layer (r_a) resistances simulated (lines), and leaf stomatal resistance recorded (symbols), at Mead, NE on 24 July and 19 August 1980. (b) Canopy temperature simulated, and air temperature recorded, on the same dates.

hourly LE_t and H_t, measured in a vertical direction, may not exactly offset R_{nt} (e.g. Fig. 4(f). There is also uncertainty in the calculation of R_{ly} as values for sky emissivity calculated according to Sellers (1965) and Idso (1981) differed under the conditions of this experiment.

There is also uncertainty in the estimation of atmospheric and canopy resistance to diffusive transfer. The equivalence of r_a for the transfer of water vapor (eqns. (12) and (19)) with that for heat (eqn. (20)) is commonly assumed, although it may in fact be higher, depending upon surface boundary conditions and large scale air circulation (McBean and Miyake, 1972). However, sensitivity of LE_c to doubled r_a under the conditions of 19 August was limited, with increases (i.e. less negative values) ranging from about 10%

in the early morning and late evening to about 1% at midday. In fact, the values recalculated with doubled r_a were closer to those recorded (Fig. 6(f)).

The estimation of r_c from Ψ_t as calculated from Ψ_c (eqns. (14)–(17)) is based on the hypothesis that the plant regulates stomatal aperture through the effect of its internal water status upon guard cell behavior. While the mathematical expression of such a hypothesis is easily parameterized from field data, evidence that r_c may be under hormonal control of the root system has also been presented (Gollan et al., 1986). The former hypothesis did, however, allow the model to reproduce the contrasting diurnal effects of R_{nc} and $q_a - q_c$ on r_c (Fig. 7(a)) as observed by Grantz and Meinzer (1990). It also allowed the model to reproduce the reduced sensitivity of r_c to $q_a - q_c$ when Ψ_s is high, as on 19 August, and when Ψ_s is low and $q_a - q_c$ is very negative as on 24 July (Fig. 7(a)), as also observed by Grantz and Meinzer (1990). It would also allow the model to reproduce the apparent decoupling between r_c and q_a when r_a is high as observed by Grantz and Meinzer (1990), because the reduced E_c calculated under these conditions (eqn. (12)) would result in higher Ψ_c (eqn. (26)) and hence Ψ_t (eqn. (15)), such that r_c would become less sensitive to changes in Ψ_t (eqn. (14)).

Even greater uncertainty exists over the estimation of crop resistance to liquid water transfer (eqn. (28)) than that over diffusive transfer. A more fundamental method for calculating the value of r_r and K_r is necessary if greater precision in these models is to be achieved.

Energy transfer over the soybean canopy recorded and simulated on 19 August was little influenced by soil water deficits as θ_w was close to field capacity in the upper part of the soil profile (Fig. 5). Daytime values of r_c and r_a simulated on this date (55 and 12 s m^{-1}) are close to those estimated by O'Toole and Real (1986) from the regression of $T_c - T_a$ on vapor pressure deficit for beans at potential transpiration (49 and 11 s m^{-1}). Simulated r_c was close to $r_{c(mn)}$ (eqn. (17)), indicating reasonable estimates of $r_c\mathrm{CO}_{2(mn)}$ from eqn. (16). Ben-Asher et al. (1989) calculated $T_c - T_a$ to be 0°C for these values of r_c and r_a when $R_{nc} = 600\,\mathrm{W\,m^{-2}}$, vapor pressure deficit = 2.0 kPa, and $T_a = 30°\mathrm{C}$, similar to conditions recorded during the early afternoon on this date (Figs. 6(a) and (b)). This canopy–air temperature gradient was closely reproduced by the model.

Energy transfer on 24 July was more influenced by soil water deficits than was that on 19 August, as indicated by values of θ_w that were close to, or lower than, the mid-point between field capacity and wilting point through the soil profile (Fig. 3). The rise in r_c during the day to 180 s m^{-1} changed the partitioning of energy transfer between LE_t and H_t in a similar way to that recorded. The ratio of simulated r_c and recorded r_l (Fig. 7(a)) was consistent with that of 0.73 estimated by Ben-Asher et al. (1989) over a range of 50 to 200 s m^{-1}. They calculated $T_c - T_a$ to be 3°C for these values of r_c and r_a when $R_{nc} = 600\,\mathrm{W\,m^{-2}}$, vapor pressure deficit = 2.0 kPa, and $T_a = 30°\mathrm{C}$, while a gradient of 2°C was estimated by the model under similar conditions (Fig. 7(b)).

The integration into the simulation model of process–level algorithms for water and energy transfer allowed it to reproduce diurnal changes in canopy water status and atmospheric energy exchange with an accuracy that was close to that of the experimental method (approximately $50\,\mathrm{W\,m^{-2}}$). Greatest discrepancies between recorded and simulated data were for LE_t during the early mornings and late evenings. The inclusion of algorithms for soil and crop hydrology allowed these changes to be reproduced at different levels of soil and crop water deficits. However, the model is based on an assumption that humidity, temperature, CO_2 and wind speed through the canopy do not deviate greatly from ambient conditions as suggested by Sinclair et al. (1976). The use of this assumption facilitated the linkage between the simulation of energy exchange and that of soil and crop hydrology by allowing a single value of Ψ_c to be used in the convergence solution of root water uptake (eqn. (26)) and of transpiration (eqn. (12)). The full linkage of a multilayer simulation of energy exchange to one of soil and crop hydrology would require the calculation of Ψ_c and water movement for each canopy layer. Such linkage would in turn require a higher resolution in our understanding of crop hydraulic conductivity than currently exists. The partial linkage of energy exchange and hydrology submodels, with the former treated at the layer level, and the latter at the canopy level, would be possible, but improvement over the model used in this study is uncertain.

ACKNOWLEDGMENTS

This research was partially supported by a grant from the National Science Foundation and utilized the CRAY-XMP/48 facility of the National Center for Supercomputing Applications at the University of Illinois in Urbana, Champaign.

REFERENCES

Acock, B., Reddy, V.R., Whisler F.D., Baker, D.N., McKinion, J.M., Hodges, H.F. and Boote, K.J., 1985. the soybean crop simulator GLYCIM: model doc. 1982, PB85 171163/AS, National Technical Information Service, Springfield, VA.

Baker, J.M. and van Bavel, C.H.M., 1988. Water transfer through cotton plants connecting soil regions of differing water potentials. Agron. J., 80: 993–997.

Baldocchi, D.D., 1982. Mass and energy exchanges of soybeans: microclimate-plant architectural interactions. Ph. D. thesis. CAMaC Progress Report 81-2. Institute of Agriculture and Natural Resources, University of Nebraska. 265 pp.

Baldocchi, D.D., 1990. Scaling water vapor and carbon dioxide exchange from leaves to a canopy: rules and tools. Workshop on Scaling Processes between Leaf and Landscape Levels. Snowbird, UT 34 pp.

Baldocchi, D.D., Hicks, B.B. and Camara, P., 1987. A canopy stomatal resistance model for gaseous deposition to vegetated surfaces. Atmos. Environ., 21: 91–101.

Baldocchi, D.D., Verma, S.B., Rosenberg, N.J., Blad, B.C., Garay, A. and Specht, J.C., 1983. Influence of water stress on the diurnal exchange of mass and energy between the atmosphere and a soybean canopy. Agron. J., 75: 543–548.

Ben-Asher, J., Meek, D.W., Hutmacher, R.B. and Phene, C.J., 1989. Computational approach to assess actual transpiration from aerodynamic and canopy resistance. Agron. J., 81: 776–782.

Campbell, G.S. 1977. An Introduction to Environmental Biophysics. Springer, NY, 159 pp.

De Willigen, P. and van Noordewijk, M., 1987. Roots, Plant Production and Nutrient Use Efficiency. Ph.D. Thesis. Agricultural University, Wageningen, Netherlands, 282 pp.

De Wit C.T., 1978. Simulation, respiration and transpiration of crops. Centre for Agricultural Publishing and Documentation. Wageningen, Netherlands, 140 pp.

Garay, A., 1981. Physical characteristics of soils of the agricultural meteorology field laboratory at Mead, Nebraska: Results of some measurements. CAMaC Progress Report 81–2. Institute of Agriculture and Natural Resources, University of Nebraska, 28 pp.

Gardner, W.R., 1960. Dynamic aspects of water availability to plants. Soil Sci., 89: 63–73.

Gollan, T., Passioura, J.B., and Munns, R., 1986. Soil water status affects the stomatal conductance of fully turgid wheat and sunflower leaves. Aust. J. Plant Physiol., 13: 459–464.

Grant, R.F., 1989a. Test of a simple biochemical model for photosynthesis of maize and soybean leaves. Agric. For. Meteorol., 48: 59–74.

Grant, R.F., 1989b. Simulation of carbon accumulation and partitioning in maize. Argon. J., 81: 563–571.

Grant, R.F., 1989c. Simulation of maize phenology. Agron. J., 81: 451–457.

Grant, R.F. 1990a. Dynamic simulation of water deficit effects upon maize yield. Agric. Systems 33: 13–39.

Grant, R.F., 1990b. The distribution of water and nitrogen in the soil–crop system: A simulation study with validation from a winter wheat field trial. Fert. Res., 27: 199–214.

Grant, R.F., Izaurralde, R.C. and Chanasyk, D.S., 1990. Soil temperature under conventional and minimum tillage. Can. J. Soil Sci., 70: 289–304.

Grant, R.F., Peters, D.B., Larson, E.M. and Huck, M.G., 1989a. Simulation of canopy photosynthesis in maize and soybean. Agric. For. Meteorol., 48: 75–92.

Grant, R.F., Frederick, J.R., Hesketh, J.D. and Huck, M.G., 1989b. Simultion of growth and morphological development of maize under contrasting water regimes. Can. J. Plant Sci., 69: 401–418.

Grant, R.F. and Lea, J.D., 1981. A technique for the measurement of osmoregulation in soybeans. Crop Prod., 10: 183–186.

Grantz, D.A. and Meinzer, F.C., 1990. Stomatal responses to humidity in sugarcane field: simultaneous porometric and micrometeorological measurements. Plant Cell Environ., 13: 27–37.

Green, R.E. and Corey, R.B., 1971. Calculation of hydraulic conductivity: a further evaluation of some predictve methods. Soil Sci. Soc. Am. Proc., 35: 3–8.

Herkelrath, W.N., Miller, E.E. and Gardner, W.R., 1977. Water uptake by plants. II. The root contact model. Soil Sci. Soc. Am. Proc. 41: 1039–1043.

Hoogenboom, G., Huck, M.G. and Hillel, D., 1987. Modification and testing of a model simulating root and shoot growth as related to soil water dynamics. Adv. Irrig., 4: 331–387.

Idso, S.B., 1981. A set of equations for full spectrum and 8 to 14 μm and 10.5 to 12.5 μm thermal radiation from cloudless skies. Water Resour. Res., 17: 295–304.

McBean, G.A. and Miyake, M., 1972. Turbulent transfer mechansims in the atmospheric surface layer. Q.J.R. Meteorol. Soc., 98: 393–398.

Norman, J.M., 1982. Simulation of microclimates. In: J.L. Hatfield and I.J. Thomason (Editors), Biometeorology and Integrated Pest Management. Academic Press, NY, pp. 65–99.

O'Toole, J.C. and Real, J.G., 1986. Estimation of aerodynamic and crop resistances from canopy temperature. Agron. J., 78: 305–310.

Reicosky, D.C., Kaspar, T.C. and Taylor, H.M., 1982. Diurnal relationship between evapotranspiration and leaf water potential of field-grown soybeans. Agron. J. 74: 667–673.

Rosenberg, N.J. and Brown, K.W., 1974. Self-checking psychrometer system for gradient and profile determinations near the ground. Agric. Meteorol., 13: 215–226.

Sellers, W.D., 1965. Physical Climatology. Univ. of Chicago Press. Chicago, IL, 272 pp.

Shaffer, M.J. and Larson, W.E. (Editors), 1987. NTRM, a Soil-Crop Simulation Model for Nitrogen, Tillage, and Crop-Residue Management. US Dept. of Agriculture Conservation Research Report, 34–1, 103 pp.

Shawcroft, R.W., Lemon, E.R., Allen, L.H., Stewart, D.W. and Jensen, S.E., 1974. The soil–plant–atmosphere model and some of its predictions. Agric. Meteorol., 14: 287–307.

Sinclair, T.R., Murphy, C.E. and Knoerr, K.R., 1976. Development and evaluation of simplified models for simulating canopy photosynthesis and transpiration. J. Appl. Ecol., 13: 813–829.

Van Bavel, C.H.M. and Hillel, D.I., 1976. Calculating potential and actual evaporation from a bare soil surface by simulation of concurrent flow of water and heat. Agric, Meteorol. 17: 453–476.

Zur. B. and Jones, J.W., 1981. A model for the water relations, photosynthesis and expansive growth of crops. Water Resour. Res., 17: 311–320.